ATP synthase is essential for high conductance but not low conductance Mitochondrial Permeability Transition

M.A. Neginskaya*, S.E. Morris, E.V. Pavlov*

Department of Molecular Pathobiology, New York University, New York, NY, USA

*Correspondence:

Maria Neginskaya, Ph.D.

Department of Molecular Pathobiology

New York University

345 East 24th Street New York, New York 10010

Tel: 212-992-7106

E-mail: mn2452@nyu.edu

and

Evgeny Pavlov, Ph.D.

Department of Molecular Pathobiology

New York University

345 East 24th Street New York, New York 10010

Tel: 212-998-9166

E-mail: ep37@nyu.edu

Abstract

A sudden increase in permeability of the mitochondrial inner membrane, known as mitochondrial permeability transition (PT), is the central event responsible for cell death and tissue damage in conditions such as stroke and heart attack. PT is caused by the opening of the Cyclosporin A (CSA) dependent calcium-induced large pore, the Permeability Transition Pore (PTP). The molecular details of PTP opening remain incompletely understood. We utilized holographic microscopy imaging to directly assess PTP induction in HAP1 living cells. We found that calcium stress caused CSA-sensitive depolarization of the mitochondrial inner membrane. PTP did not occur until after nearly complete mitochondrial membrane depolarization. In cells lacking c and δ subunits of the ATP synthase, we observed CSA-sensitive membrane depolarization but not high-conductance PTP. We propose that PTP activation occurs as a two-phase process, with the initial membrane depolarization followed by the second phase of large pore opening that requires ATP synthase.

Introduction

The low permeability of the mitochondrial inner membrane is an essential condition for efficient coupling between respiratory chain activity and phosphorylation of ADP by ATP synthase (*1, 2*). An increase in the permeability of the inner membrane would lead to mitochondrial membrane depolarization, uncoupling of the oxidative phosphorylation, and mitochondrial energy failure. It is generally accepted that such an increase in permeability, known as permeability transition (PT) is a critical contributor towards cell death in a wide range of acute stress conditions associated with hypoxic-ischemic injuries (*3*). PT is caused by the activation of the PT pore (PTP) at the mitochondrial inner membrane. The molecular mechanisms of PTP are not entirely understood and are subject of intensive investigation (*4-10*).

Despite the large arsenal of methods available to experimentally study PTP, the number of direct assays is surprisingly limited. The signature feature of PTP is an unselective increase in membrane permeability to ions and other molecules up to 1.5 kDa in size, which can be blocked by Cyclosporin A (CSA) (*11*). PTP activation causes three events that can be detected experimentally: mitochondrial membrane depolarization, calcium release from the mitochondrial matrix, and optical density (OD) decrease due to solute exchange, which in isolated mitochondria is accompanied by swelling (*12*). Out of these three events, only OD change is specific to the high-conductance PTP since depolarization and calcium release can be caused by other mechanisms of membrane permeability increase not necessarily related to the PTP. As such, OD assays (also known as “light-scattering” or “swelling” assays) remain the golden standard in studies of PTP as the only unambiguous method. This method has been extensively used in experiments with isolated mitochondria for over the past five decades. It relies on the measurements of changes in the optical properties of the mitochondrial matrix, as during solute equilibration mitochondria become progressively more and more transparent. Using the holographic imaging approach, we have been able to extend this method to the living cells. Holographic imaging is sensitive to the changes of the refractive index (RI). RI reflects the OD of the object and shows how fast the light propagate through the object. By estimation of the delay of the light passing through the object with higher OD (and RI) the holographic microscope can reconstruct the shape of the object. In our experiments, which rely on the measurement of the differences between RIs of the mitochondrial matrix and cytoplasm, mitochondrial PTP induction caused equalization of optical densities and disappearance of the organelles from holographic image (RI image). We have found that in wild-type HAP1 cells calcium-induced high-conductance PTP is preceded by membrane depolarization, while in the ATPase c and δ subunits deficient cells, there is no large scale mitochondrial permeabilization despite membrane depolarization. Our work confirms the applicability of this novel imaging technique towards studying PTP in intact cells and provides direct experimental support for the idea of the essential role of ATP synthase in the high-conductance PTP.

Materials and methods

Cell culture

Immortalized cell lines HAP 1 and MEF were used for holographic imaging assay. The cells were cultured as described previously (*6, 7*). Briefly, HAP 1 cells were grown Iscove's Modified Dulbecco's Medium (IMDM), supplemented with 10% FBS, 10 mL per L of Antibiotic Antimycotic Solution Penicillin/Streptomycin/Amphoterichin B; Sigma Aldrich) and 2 mM L-Glutamine. MEF cells were grown in high glucose Dulbecco's Modified Eagle Medium (DMEM) supplemented with 10% FBS, 10 mL per L of Antibiotic Antimycotic Solution Penicillin/Streptomycin/Amphoterichin B (Sigma Aldrich), 2 mM L-Glutamine, non-essential amino acids. Both cell lines were maintained in a humidified cell incubator, at 37°C under a 5% CO2 atmosphere. HAP 1 Δ (c+δ) cell line that lacks c and δ-subunits of ATP synthase were used for the study of the role of ATP synthase in high-conductance PTP.

Holographic and Fluorescent Imaging

The cells were plated on poly-D-lysine coated glass coverslips 24 hours before imaging to reach the confluency of 70-90 %. Before the experiment the coverslips with the cells were places in the imaging chamber and washed with Hank's Balanced Salt Solution (HBSS, Gibco). TMRM fluorescent probe (Invitrogen) was used for estimation of mitochondrial membrane potential. Cells were incubated with 40 nM of TMRM for 15 min in room temperature in the darkness. Recording media contained 40 nM of TMRM. Ferutinin (20 µM for HAP 1; 30 µM for MEF; Sigma Aldrich) was used to induce calcium-induced PT. Holographic (RI) images and TMRM signal were acquired every 15 seconds with aid of 3D Cell Explorer-fluo (Nanolive, Switzerland) equipped with 60X objective. Protonophore FCCP (10 µM; Sigma Algrich) was used at the end to observe the drop of membrane potential and normalize the TMRM signal.

Data processing and analysis

Fiji ImageJ was used to process holographic reconstructions. Multipage TIF files were prepared as described in (*13*). Plain RI images were reconstructed as a Z-stack projection from the volume of the cell that contained mitochondria. Ilastik, the interactive learning and segmentation toolkit, was used for mitochondrion segmentation. After being trained by the user, Ilastik tool creates the probability map of pixels that relate to mitochondria and based on the probability, classify them as mitochondria (Fig. S1A, S3B). Segmented images were converted to a binary image with Fiji "Make binary" tool. Resulted image is shown in Figure S1C.

To analyze the mitochondrial membrane permeabilization, we estimated the decrease in the refractive index (RI) of mitochondria by the decrease of the area occupied by mitochondria in reconstructed images. To do so, the regions of interest (ROIs) with functional mitochondria with maintained membrane potential were selected manually from the corresponding fluorescent images of cells labeled with TMRM (Fig. S1C, S1D).

These ROIs were used to estimate changes in membrane potential and applied to binary segmented masks created as described above. Next, the area occupied by mitochondria was estimated in selected ROIs in each time frame. The decrease of the area indicated the decrease of mitochondrial RI and, thus, mitochondrial permeabilization. The half-time of depolarization and the half-time of mitochondrial permeabilization were estimated with Origin 2021b by using sigmoidal fit (Fig. 2F, Fig. S2).

Single mitochondrion tracking was performed manually by selecting the mitochondrion areas in RI images frame by frame. The same areas were used in corresponding TMRM fluorescent images to track the changes in mitochondrial membrane potential.

Seahorse assay

Analysis of mitochondrial functions in HAP 1 WT and HAP 1 Δ(c+δ) cells was performed on Seahorse XFe24 (Agilent Technologies, USA) as described previously (*14*). Briefly, cells were plated on Seahorse XFe24 Cell culture 24-wells microplates 24 hours before experiment to reach the confluency 70-80% according to Agilent Technologies recommendations.

The night before the experiment, the cartridge containing the sensors was hydrated with 1 ml of XF Calibrant Solution and kept overnight in a CO_2-free incubator. The day of the experiment, cells were washed with Seahorse XF DMEM medium that contained 1 mM pyruvate, 2 mM glutamine, and 10 mM glucose and incubated for 1 h in the CO_2-free incubator (hypoxia). The cartridge was loaded with 30 µM of Ferutinin, 1 µM of FCCP and 0.5 µM of rotenone/antimycin A (Rot/AA) to the ports A, B and C accordingly to measure OCRs and ECARs. All the drugs were dissolved to the working concentrations using the Seahorse XF DMEM medium. Subsequently, the cells were loaded onto the analyzer and the measurements were conducted. The obtained data was exported and analyzed using the Seahorse Wave Desktop Software, which was downloaded from the Agilent Technologies' website.

Statistics

Origin 2021b software (OriginLab, Massachusetts, USA) was used for data presentation, analysis and statistics. All the data presented as Mean±SEM. The exact numbers of experiments (N) and cells (n) analyzed are mentioned in corresponding parts of the text. ANOVA and t-test were used to verify statistical significance.

Results

Calcium overload induces CSA-sensitive mitochondrial depolarization that is accompanied by high amplitude membrane permeabilization

Holographic imaging achieves the resolution of intracellular structures that are not visible when using conventional bright-field microscopy. In a holographic image, the picture is reconstructed based on the differences in the refractive indexes of different areas of the cell rather than on light absorbance (*13*). Figure 1 illustrates that holographic imaging allows one to distinguish inner cellular structures that are not visible when bright-field imaging is applied (compare images on Figs. 1A and 1B). As shown in the RI image in Figure 1B, mitochondria (arrows) were visualized directly inside the living cell without the use of fluorescent labels. The identity of these structures was confirmed by the fluorescent probe TMRM, which selectively stains polarized mitochondria (Fig. 1C). Overlay of the RI and TMRM images allowed us to clearly distinguish and track structures representing mitochondria (Fig. 1 D-F).

We measured the response of mitochondria to the addition of the calcium ionophore ferutinin. Ferutinin electrogenically delivers calcium into mitochondria and induces CSA-sensitive membrane depolarization, indicating PTP activation (*15*). We used an HAP 1 cell line that has been verified by previous studies to be a robust cell culture model for the investigation of the molecular details of PTP (*5, 6, 8, 16*). We simultaneously monitored the membrane potential and RI of the mitochondrial regions (Fig. 2 and Fig.S3). Figs 2A and 2B show representative RI images of the cells before and after induction of PTP with ferutinin (20 µM) as well as corresponding processed images (Fig. 2C, D) which used a specific threshold (see Materials and Methods) to identify regions with higher RI. As can be seen from the figures, activation of PTP leads to the disappearance of the mitochondrial structures (verified by TMRM fluorescence, not shown) from the RI images, which is consistent with the equilibration of the solutes and thus optical densities (and RI) between the matrix and cytoplasm. Drop in RI of mitochondria coincided with membrane depolarization that was detected by the decrease in TMRM signal (Fig. 2 E, F; N = 5; n = 83). In control experiments, when depolarization was induced by the protonophore FCCP without PTP induction, mitochondria remained intact and easily recognizable in the RI images (Fig. 3 and Fig. S3, N=3; n=55). Both membrane depolarization and RI drop were prevented by the addition of CSA (Fig. 4; N=4; n=89). These data demonstrate that non-selective mitochondrial membrane permeabilization can be directly detected in the living cells and that this increase in permeability is indicative of the activation of the high-conductance PTP. Importantly, similar effect of ferutinin-induced (30 µM) depolarization and RI drop was also seen in the MEF cells, suggesting the applicability of the method towards different cell types (Fig. S4, N=3; n=39).

Mitochondrial depolarization occurs before high amplitude membrane permeabilization.

Experiments and analysis shown in Fig. 2 were performed on the regions of interest which included a large number of mitochondria. These results demonstrate the clear correlation in time for the course of mitochondrial depolarization and a decrease in RI, but also shows the slight time offset between these two processes. We aimed to gain further insight into the relationship between depolarization and permeabilization by analysing them at the single mitochondrion level. Figure 5 shows the result of simultaneous analysis of the dynamics of mitochondrial membrane potential and non-selective permeabilization performed at the level of a single mitochondrion. Here, we traced individual mitochondria using both RI and TMRM readouts from the moment before treatment where mitochondria were functional (Fig. 5A) and visible on RI image (Fig. 5B) until the mitochondrial disappearance (Fig. 5D). The specific organelles RI were tracked throughout the duration of the experiment frame by frame as shown in Fig. 5C for 2 selected mitochondria. TMRM signal was detected at corresponding areas of fluorescent images (Fig. 5A). As shown in Figures 5E and 5H, ferutinin caused a gradual decrease in the membrane potential. Interestingly, despite significant membrane depolarization, the RI of individual mitochondrion stayed largely undisturbed and individual mitochondrion remained clearly visible (Figs. 5E and 5F for mitochondrion 1, and 5H and 5I for mitochondrion 2). However, mitochondria rapidly disappeared from RI images when depolarization was nearly complete (Figs 5E and 5G for mitochondrion 1, and 5H and 5J for mitochondrion 2). The membrane potential of individual mitochondrion at the moment of organelle disappearance from RI image was 15 ± 6 % of the initial potential level (Fig. 5K, left panel, n=10). The average time delay from the start of depolarization until the disappearance of the individual mitochondrion was 150 ± 20 seconds (Fig. 5K, right panel, n=10; $p<0.001$). Overall, individual mitochondrion analysis showed that almost complete depolarization occurred prior to the onset of non-selective large-scale membrane permeabilization, and on average, the permeabilization was delayed by 150 ± 20 seconds from the beginning of the depolarization (Fig. 5K, n=10; $p<0.001$). Altogether these experiments indicated that initial depolarization occurred prior to high-conductance PTP activation. This is a new insight that suggests that the high-conductance PTP is not the cause of membrane depolarization.

Cells lacking assembled ATP synthase undergo CSA-sensitive depolarization but not high amplitude membrane permeabilization

It has been suggested that ATP synthase plays an important role in the PTP. However, recent studies using a double knockout HAP1 mutant (HAP1 Δ (c+δ)), lacking c and δ subunits and, consequently, making them devoid of the assembled ATP synthase, show that these mitochondria can still undergo calcium-induced depolarization in the intact cells when stimulated with ferutinin (*5*). Using holographic imaging, we investigated the relationship between the calcium-induced depolarization and high-amplitude mitochondrial permeabilization. As demonstrated in Figure 6, unlike wild-type cells, HAP1 Δ (c+δ) cells did not undergo high amplitude permeabilization, despite membrane depolarization (Fig. 6 and Fig. S3; N=5, n=107). This suggests that the assembled ATP

synthase is required for the development of the high-conductance PTP but is not involved in the initial membrane depolarization that is triggered by the addition of ferutinin. Importantly, this initial depolarization was inhibited by CSA in both WT and HAP1 Δ (c+δ) (Fig. 4, and Fig. S5), suggesting that it represents one of the stages of the PTP activation process. On an interesting note, in the WT cells CSA prevented depolarization but caused extensive mitochondrial fragmentation. Despite this fragmentation, mitochondria did not undergo high amplitude permeabilization (Fig. 4).

The lack of the high amplitude permeabilization was further confirmed by measurements of the effects of the ferutinin on mitochondrial respiration using Seahorse metabolic flux analyzer. As can be seen from Fig. S6A, ferutinin caused rapid loss of mitochondrial function in the WT cells consistent with what would be expected from the high-conductance PTP activation and loss of the respiratory chain substrates. On the contrary, the same amount of ferutinin transiently stimulated mitochondrial respiration in the HAP1 Δ (c+δ) cells (Fig. S6B). This stimulation of the respiration is consistent with the observation that despite depolarization, mitochondrial of these mutant cells remained structurally intact which allowed them to (at least transiently) maintain respiratory activity. The effects of the addition of ferutinin on the respiratory function for both cell types were blocked by CSA, confirming that both processes, membrane depolarization and high-amplitude mitochondrial permeabilization, are related to PTP.

Discussion

Traditionally, a functional assay of the PTP in intact cells relies on the fluorescent measurements of the mitochondrial parameters. In most cases, PTP can be experimentally identified as a calcium-induced CSA-sensitive membrane depolarization and/or calcium release, both of which can be detected fluorometrically in the intact cells (*17, 18*). Notably, these methods do not necessarily indicate activation of the high-conductance PTP. To our knowledge, the only fluorescent method specifically geared towards PTP is monitoring the calcein release from the mitochondria (*19*), where calcein release would indicate the opening of the large pore. However, this method has limitations since calcein release does not necessarily indicate high amplitude PTP and can occur even in non-stress conditions due to the pore flickering. The method described here provides a direct assay that does not require the use of any probe and that relies on the definitive feature of PTP, which is the equilibration of the solutes across the mitochondrial membrane.

Further, unlike in experiments involving isolated mitochondria in the population, we could monitor optical density in the single mitochondrion. This is an important advantage as changes in light scattering in the population might not necessarily reflect complete swelling of individual organelles, but rather gradual changes in “average” light scattering across the whole population. We anticipate that this method will help to clarify many details in the PT at the level of intact cells and resolve some current controversies.

One important aspect of PTP which this new method would allow for the clarification of, is the ability to more accurately estimate the relationship between PTP and mitochondrial swelling. It is known that, following calcium treatment, isolated mitochondria eventually swell and, in the literature, generally the terms “light-scattering” and “swelling” assay are used interchangeably. However, prior to PTP opening, mitochondria are perfectly osmotically and oncotically balanced with the surrounding medium. Opening of the non-selective PTP - which allows flux of molecules of up to 1.5 kDa in size - would definitely cause a drop in OD due to the equilibration of the matrix and medium content. At the same time, however, this solute exchange should not necessarily lead to swelling in the living cell. The oncotic pressure of non-permeable proteins would remain balanced, as it was prior to PTP, while permeable molecules would exchange freely, leaving the net accompanying water flux unchanged. Single mitochondria RI imaging will help to clarify if swelling is indeed the direct consequence of the PTP opening, or if swelling occurs at the later stages of mitochondrion demise.

The advantage of being able to monitor OD in real-time with single organelle resolution is evident from our experiments with simultaneous monitoring of the OD in relation to the mitochondrial membrane potential. As shown in Figure 5, during the induction of the PTP by the addition of calcium, we detected that at the first stage, mitochondria undergo membrane depolarization, followed by a second stage of the PTP characterized by high amplitude membrane permeabilization. This observation

challenges the widely accepted view that calcium-induced PTP is a cause of membrane depolarization (*20*). Our data suggest that the initial step of PTP activation is likely the opening of the lower conductance channel that is sufficient to depolarize mitochondria. This occurs prior to the activation of the high-conductance PTP which is required for mitochondrial swelling (as seen in the isolated mitochondria). The fact that CSA was able to prevent the depolarization step but caused mitochondrial fragmentation (Fig. 4) suggests an exciting possibility that this initial step might be beneficial for cell protection against stress. Its inhibition by CSA, which preserves mitochondrial function might not necessarily be protective at the cellular level.

The molecular mechanisms of PT activation and function remain incompletely understood. It is very likely that physically PT can occur through several pathways. One of the key challenges in the field is understanding the role of the ATP synthase in this process. Compelling evidence from several independent laboratories supports the models that involve the ATP synthase complex, which could be transformed into the high-conductance pore (*4, 10*). Equally compelling evidence suggests that, at the level of intact cells and isolated mitochondria from the mutant cells lacking an assembled ATP synthase, PTP is indistinguishable from that seen in wild-type cells (*5*). In both cases, calcium treatment through the addition of ferutinin caused calcium release and membrane depolarization that was inhibited by CSA. Here, using the same cell model that lacked the assembled ATP synthase, we observed both phenomena with a notable difference – mitochondria in these mutant cells did not undergo high amplitude permeabilization. Thus, the direct assay confirms the presence of PTP in both cell types at the level of intact cells. However, importantly, ATP synthase is essential for the development of the high-conductance PTP.

In summary, the two phenomena observed in our experiments suggest the presence of a low-conductance mode of PTP, which occurs independent of the ATP synthase required for the high-conductance mode of PTP. These observations are consistent with previous studies on cells lacking a c subunit in containing a channel that, similar to PTP, is calcium-activated and CSA-sensitive, but has significantly smaller conductance compared to the classical high-conductance PTP (*8*). We hypothesize that PTP development might be a two-channel phenomenon. Both of these channels are sensitive to CSA, but their activation occurs at different time points in the process. The lack of the high amplitude PTP in the HAP1 Δ (c+δ) cells opens an exciting possibility that the two steps of PTP might involve different molecular structures. It is tantalizing to suggest that selectively targeting ATP synthase might help to identify compounds that would prevent mitochondrial high amplitude permeabilization but allow a protective depolarization step, which would prevent mitochondria from excessive fission.

Acknowledgements

We thank Prof. Mike Murphy (University of Cambridge, UK) and Prof. Nickolay Brustovetsky (University of Indiana, USA) for critical reading of the manuscript and fruitful discussion and Prof. John Walker (University of Cambridge, UK) for providing HAP 1 cell lines. This work was supported by grants # R35GM139615 and R01GM115570 from NIGMS (to E.P.) and AHA Postdoctoral fellowship (to M.N.).

Figures

Figure 1. Holographic imaging allows monitoring of mitochondria in the living cells label-free. A. Bright field image of immortalized HAP-1 cell culture. B. Holographic image of the same area of the cells. No label was used. C. Overlay, showing colocalization between RI (E) and TMRM images (F). Areas with live mitochondria that maintain membrane potential are stained. Arrows point to mitochondrial areas. D, E, F. Enlarged images of the region shown in the white box on panel B. D. Staining with TMRM reflecting mitochondrial membrane potential. Scale bar – 10 µm for A-C; 5 µm for D-F.

Figure 2. Simultaneous detection and quantification of the mitochondrial depolarization (TMRM, red) and permeabilization (RI) in the HAP 1 WT living cells. Panels A and B show holographic images of the cells before and 6 minutes after the addition of ferutinin (20 µM). Regions with distinct mitochondrial networks indicated by arrows. Note the disappearance of the mitochondria at panel B. Panels C and D show processed images A and B that allow specific detection of the decrease in RI of mitochondrial regions. E, F time-dependent changes of TMRM and RI signals of the mitochondrial regions. E, F. Representative of 5 independent experiments. F. Each data point represents value collected from different mitochondrial regions within the same field of view. Scale bar – 5 µm.

Figure 3. Mitochondrial structure in HAP 1 WT cells remains intact following membrane depolarization induced by the protonophore FCCP (10 µM), which does not cause PTP. Holographic and fluorescent (TMRM) image of mitochondria before (A, C) and after (B, D) addition of the FCCP (10 µM). E. Time dependence of the membrane depolarization and RI measurements. Note that the refractive index remained unchanged, indicating a lack of mitochondrial permeabilization. Scale bar – 5 µm.

Figure 4. Mitochondrial depolarization in HAP 1 WT cells was inhibited by CSA (2 µM). Holographic and fluorescent (TMRM) images of cells before (A, B) and after (C,D) the addition of ferutinin (20 µM). Note that mitochondrial depolarization occurred only after the addition of FCCP (E, F). G. Time course of the membrane potential changes. Scale bar – 5 µm.

Figure 5. Monitoring time-dependent membrane depolarization and high-amplitude permeabilization in HAP 1 WT cells at the level of a single mitochondrion. A-D. Fluorescent (TMRM) (A) and holographic images of the cell at the beginning of the experiment (B,C) and following ferutinin addition (D). Labels on panel C show the selection of two representative mitochondria. Scale bar – 5 µm. E, H. time dependence of the TMRM fluorescence from the mitochondria #1 and #2 (see panel C). F, G images correspond to the time points marked by arrows at panel E for mitochondrion #1; note the disappearance of mitochondrion from the panel G. H-J analysis similar to the panels E-G for the mitochondrion #2. K. The relationship between mitochondrial depolarization and permeabilization at the level of single mitochondrion. Left panel, the level of the residual membrane potential at the moment of mitochondrial permeabilization (n=10).

Right panel, the time delay between the offset of depolarization and permeabilization ($n=10$; $p<0.001$; t-test for null-hypothesis).

Figure 6. Lack of high amplitude permeabilization despite membrane depolarization in HAP1 Δ (c+δ) cells. Holographic and florescent (TMRM, red) images of cells before (A, C) and after (B, D) the addition of ferutinin (20 µM). Time dependence of the membrane depolarization and refractive index measurements. Note that refractive index remained unchanged, indicating a lack of mitochondrial membrane permeabilization. Scale bar – 5 µm.

References

1. P. Mitchell, Coupling of phosphorylation to electron and hydrogen transfer by a chemi-osmotic type of mechanism. *Nature* **191**, 144-148 (1961).
2. P. D. Boyer, The ATP synthase--a splendid molecular machine. *Annu Rev Biochem* **66**, 717-749 (1997).
3. P. Bernardi *et al.*, The mitochondrial permeability transition from in vitro artifact to disease target. *FEBS J* **273**, 2077-2099 (2006).
4. V. Giorgio *et al.*, Dimers of mitochondrial ATP synthase form the permeability transition pore. *Proc. Natl. Acad. Sci. U. S. A* **110**, 5887-5892 (2013).
5. J. Carroll, J. He, S. Ding, I. M. Fearnley, J. E. Walker, Persistence of the permeability transition pore in human mitochondria devoid of an assembled ATP synthase. *Proc Natl Acad Sci U S A* **116**, 12816-12821 (2019).
6. J. He *et al.*, Persistence of the mitochondrial permeability transition in the absence of subunit c of human ATP synthase. *Proc Natl Acad Sci U S A* **114**, 3409-3414 (2017).
7. J. Karch *et al.*, Inhibition of mitochondrial permeability transition by deletion of the ANT family and CypD. *Sci Adv* **5**, eaaw4597 (2019).
8. M. A. Neginskaya *et al.*, ATP Synthase C-Subunit-Deficient Mitochondria Have a Small Cyclosporine A-Sensitive Channel, but Lack the Permeability Transition Pore. *Cell Rep* **26**, 11-17 e12 (2019).
9. M. Bonora *et al.*, Role of the c subunit of the FO ATP synthase in mitochondrial permeability transition. *Cell Cycle* **12**, 674-683 (2013).
10. K. N. Alavian *et al.*, An uncoupling channel within the c-subunit ring of the F1FO ATP synthase is the mitochondrial permeability transition pore. *Proc. Natl. Acad. Sci. U. S. A* **111**, 10580-10585 (2014).
11. M. Crompton, H. Ellinger, A. Costi, Inhibition by cyclosporin A of a Ca2+-dependent pore in heart mitochondria activated by inorganic phosphate and oxidative stress. *Biochem. J* **255**, 357-360 (1988).
12. A. Y. Baev, P. A. Elustondo, A. Negoda, E. V. Pavlov, Osmotic regulation of the mitochondrial permeability transition pore investigated by light scattering, fluorescence and electron microscopy techniques. *Anal Biochem* **552**, 38-44 (2018).
13. Y. Cotte *et al.*, Marker-free phase nanoscopy (vol 7, pg 113, 2013). *Nat Photonics* **7**, 418-418 (2013).
14. M. Nichols *et al.*, Global ablation of the mitochondrial calcium uniporter increases glycolysis in cortical neurons subjected to energetic stressors. *J Cereb Blood Flow Metab* **37**, 3027-3041 (2017).
15. A. Y. Abramov, M. R. Duchen, Actions of ionomycin, 4-BrA23187 and a novel electrogenic Ca2+ ionophore on mitochondria in intact cells. *Cell Calcium* **33**, 101-112 (2003).
16. J. He, J. Carroll, S. Ding, I. M. Fearnley, J. E. Walker, Permeability transition in human mitochondria persists in the absence of peripheral stalk subunits of ATP synthase. *Proc Natl Acad Sci U S A* **114**, 9086-9091 (2017).
17. M. R. Duchen, Roles of mitochondria in health and disease. *Diabetes* **53 Suppl 1**, S96-102 (2004).
18. M. Bonora *et al.*, Comprehensive analysis of mitochondrial permeability transition pore activity in living cells using fluorescence-imaging-based techniques. *Nat Protoc* **11**, 1067-1080 (2016).
19. V. Petronilli *et al.*, Transient and long-lasting openings of the mitochondrial permeability transition pore can be monitored directly in intact cells by changes in mitochondrial calcein fluorescence. *Biophys. J* **76**, 725-734 (1999).

20. M. Zoratti, I. Szabo, The mitochondrial permeability transition. *Biochim. Biophys. Acta* **1241**, 139-176 (1995).

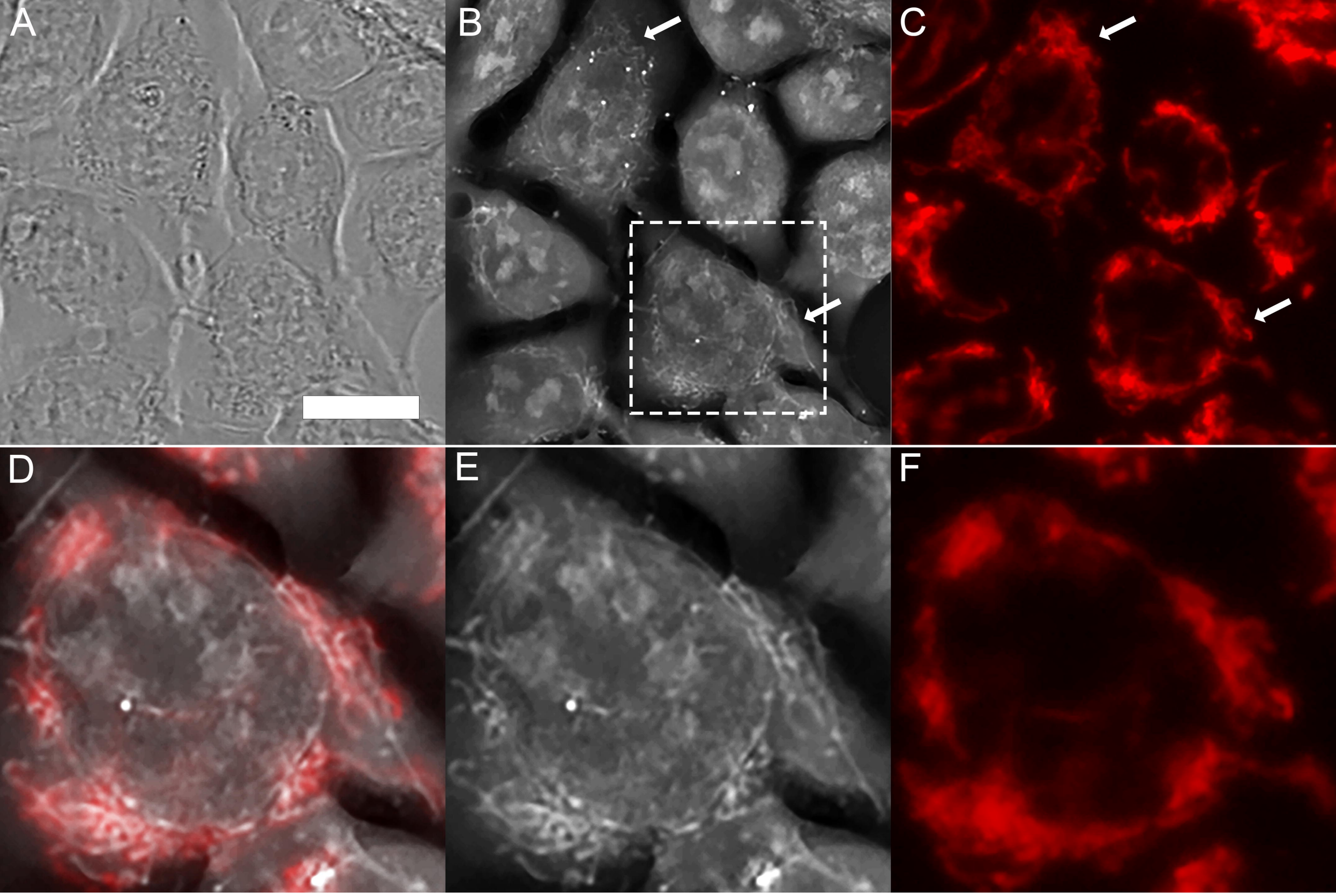
A
B
C
D
E
F

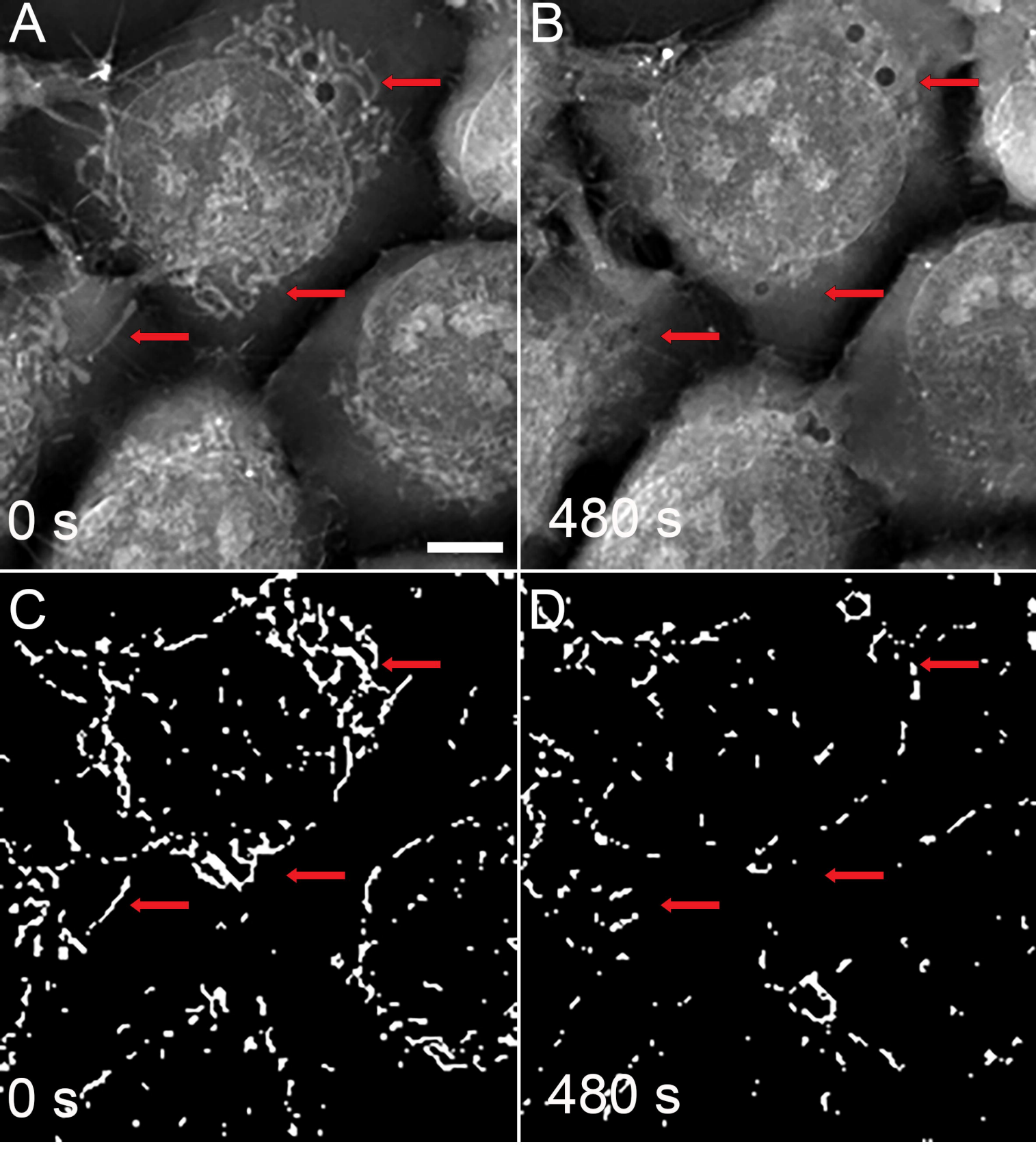
A
0 s
B
480 s
C
0 s
D
480 s

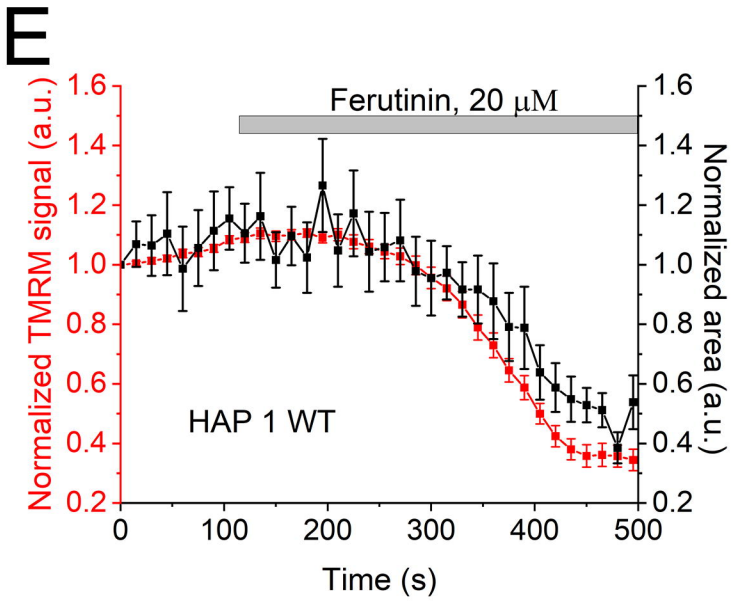
E
Ferutinin, 20 μM
HAP 1 WT
Normalized TMRM signal (a.u.)
Normalized area (a.u.)
Time (s)
0
100
200
300
400
500
0.2
0.4
0.6
0.8
1.0
1.2
1.4
1.6

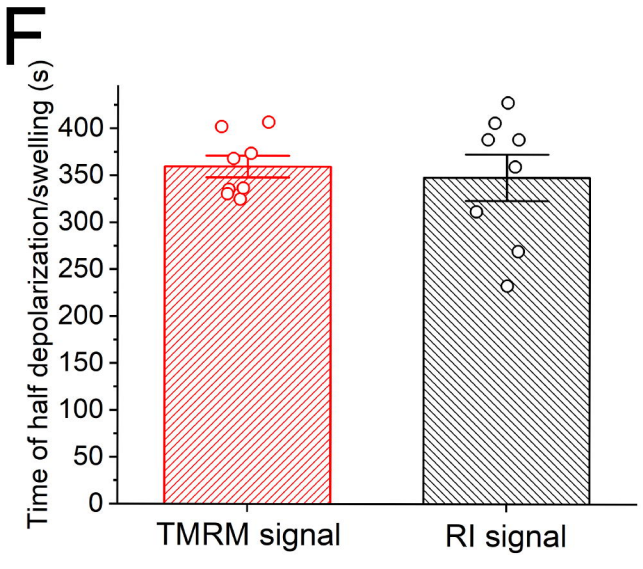
F
Time of half depolarization/swelling (s)
0
50
100
150
200
250
300
350
400
TMRM signal
RI signal

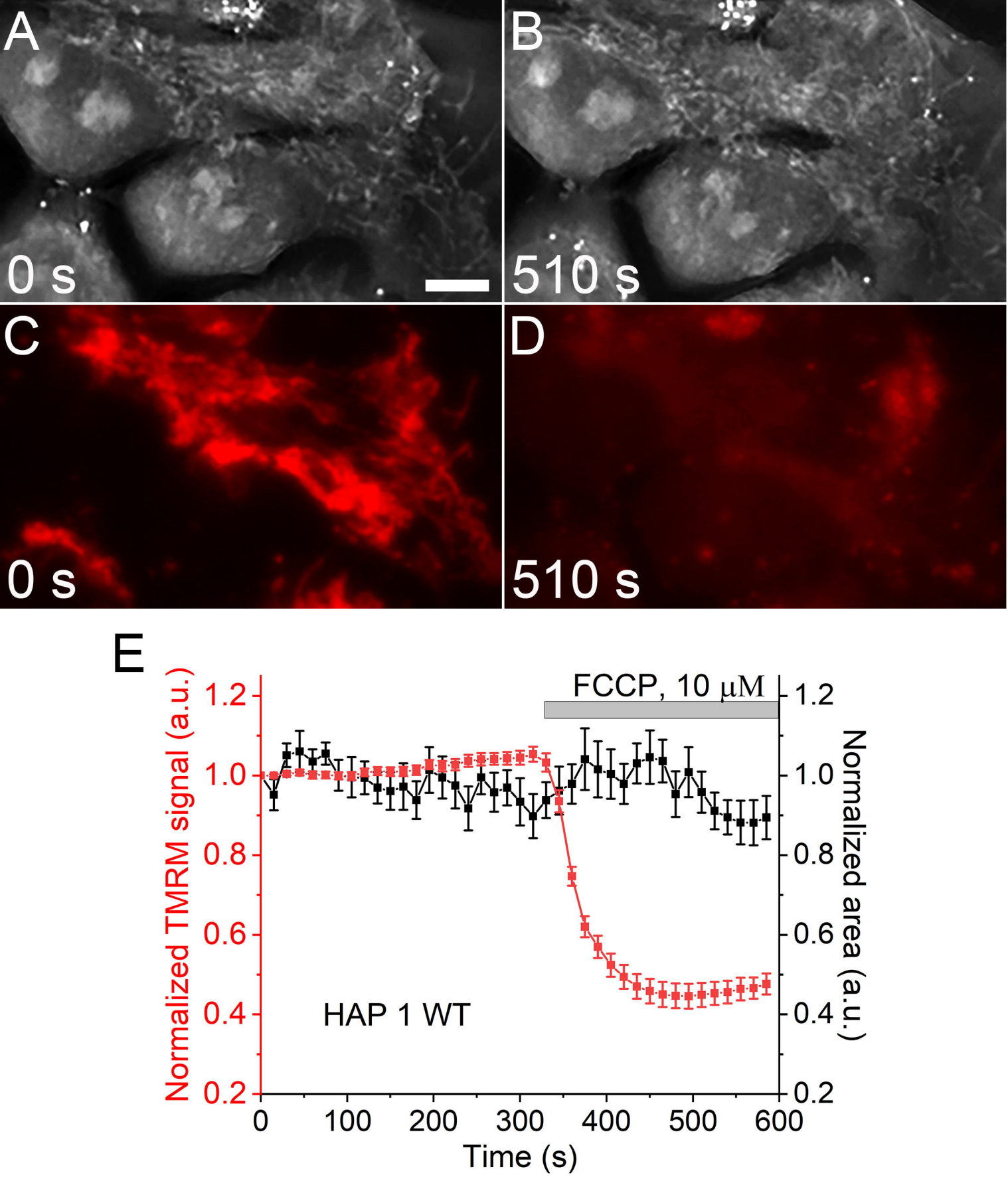
A
0 s
B
510 s
C
0 s
D
510 s
E
FCCP, 10 μM
HAP 1 WT
Normalized TMRM signal (a.u.)
Normalized area (a.u.)
Time (s)
0.2
0.4
0.6
0.8
1.0
1.2
0
100
200
300
400
500
600

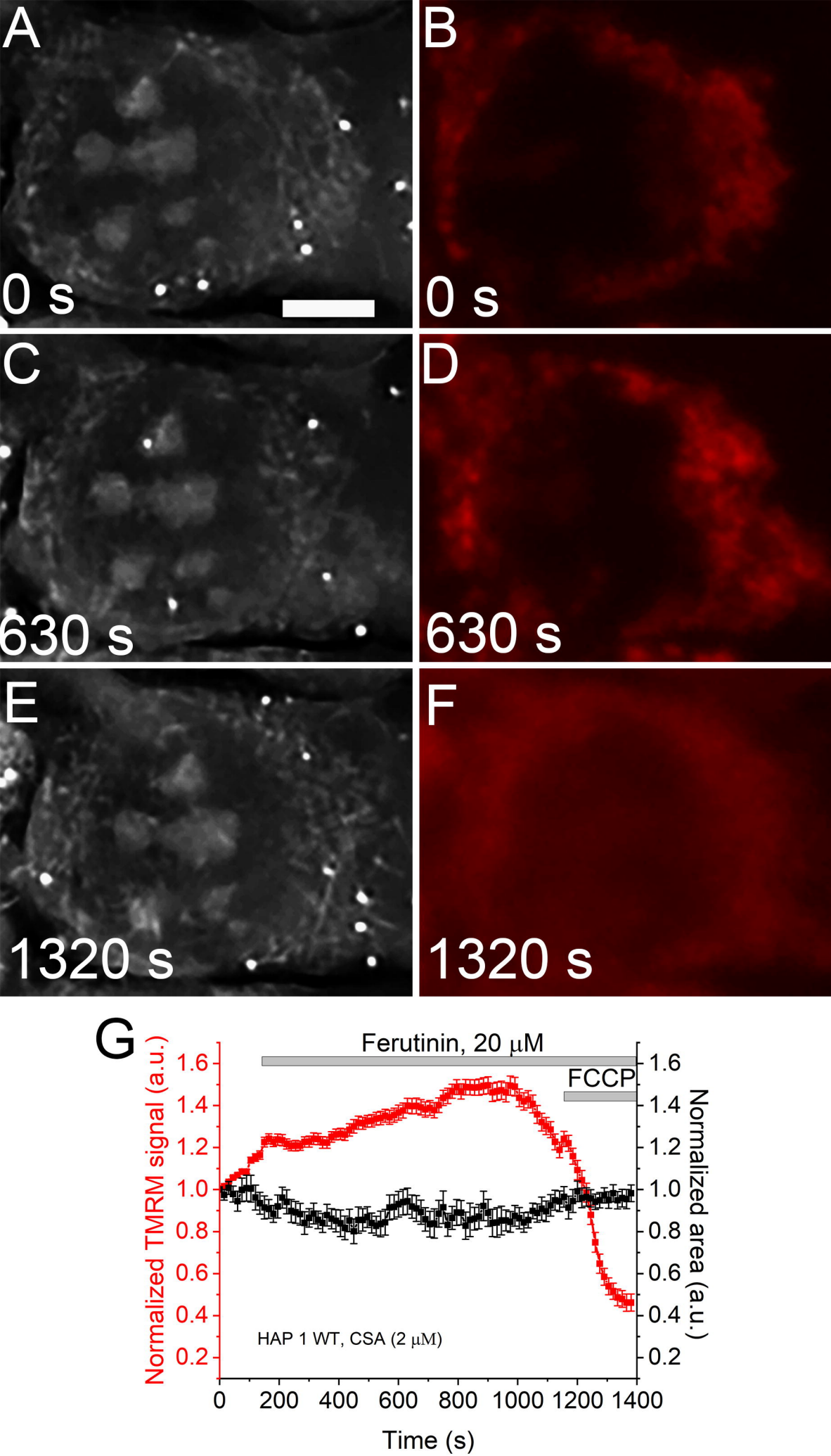
A
0 s
B
0 s
C
630 s
D
630 s
E
1320 s
F
1320 s
G
Ferutinin, 20 μM
FCCP
HAP 1 WT, CSA (2 μM)
Normalized TMRM signal (a.u.)
Normalized area (a.u.)
Time (s)
0.2
0.4
0.6
0.8
1.0
1.2
1.4
1.6
0
200
400
600
800
1000
1200
1400

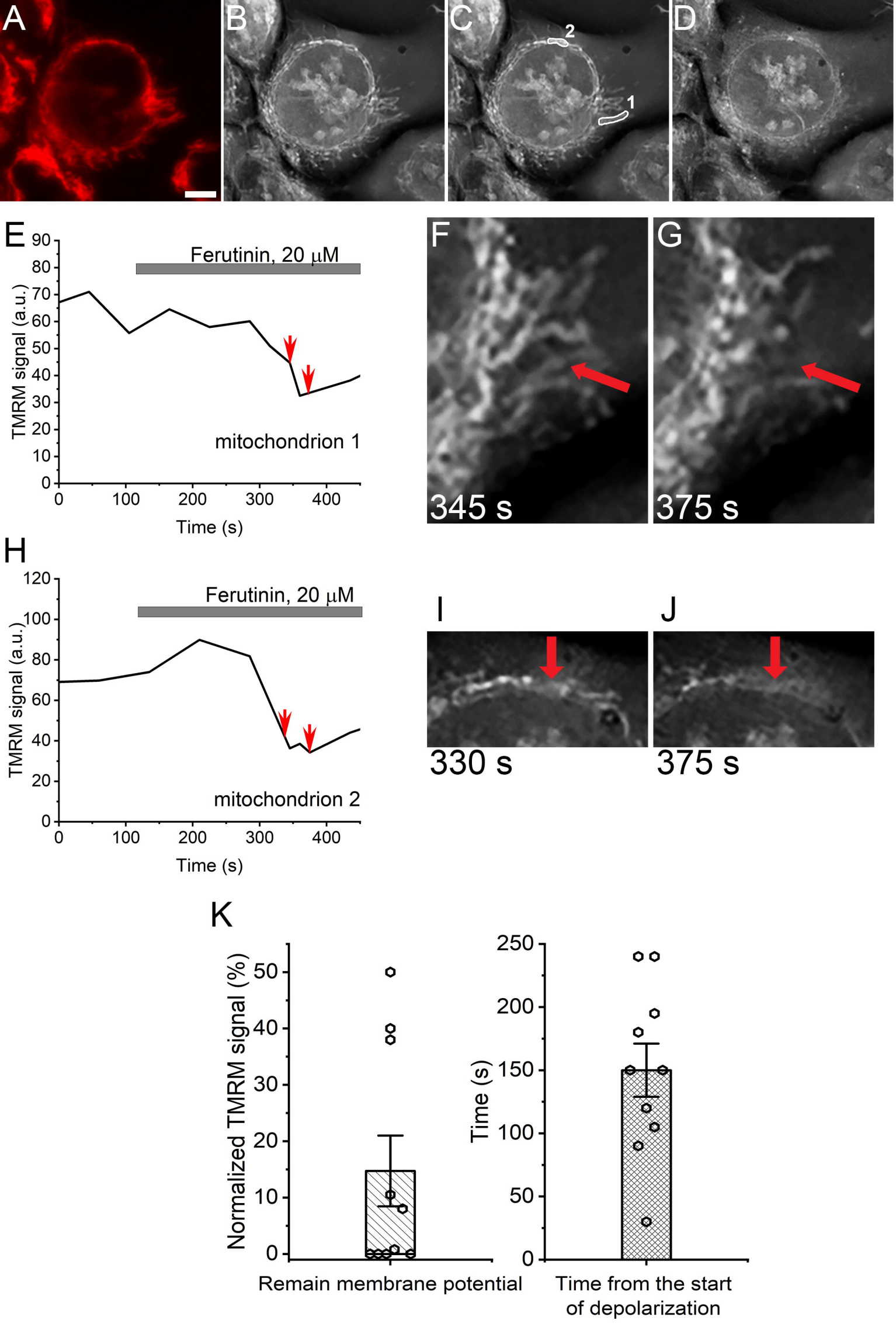
A
B
C
2
1
D
E
Ferutinin, 20 μM
TMRM signal (a.u.)
mitochondrion 1
Time (s)
F
G
345 s
375 s
H
Ferutinin, 20 μM
TMRM signal (a.u.)
mitochondrion 2
Time (s)
I
J
330 s
375 s
K
Normalized TMRM signal (%)
Time (s)
Remain membrane potential
Time from the start of depolarization

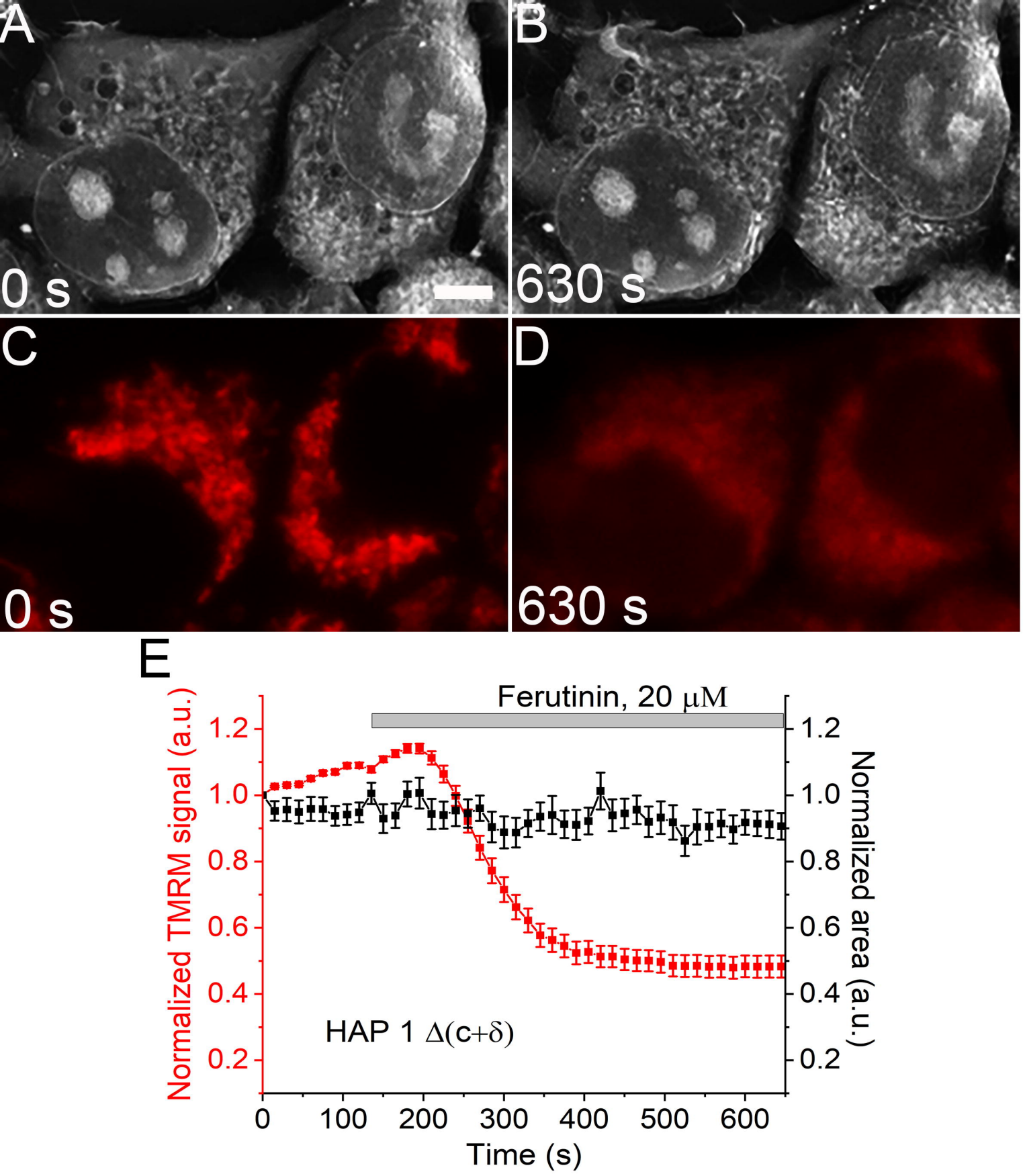
A
0 s
B
630 s
C
0 s
D
630 s
E
Ferutinin, 20 μM
Normalized TMRM signal (a.u.)
Normalized area (a.u.)
HAP 1 Δ(c+δ)
Time (s)
0
100
200
300
400
500
600
0.2
0.4
0.6
0.8
1.0
1.2